Electronic Supplementary Information

Coexistence of self-reduction from Mn^{4+} to Mn^{2+} and the elastico-mechanoluminescence in diphase $KZn(PO_3)_3:Mn^{2+}$

Huimin Chen,[a] Liwei Wu,[a] Fang Bo,[a] Jikang Jian,[b] Li Wu,*[a] Hongwu Zhang,*[c] Lirong Zheng,*[d] Yongfa Kong,[a] Yi Zhang[e] and Jingjun Xu[a]

[a]Key Laboratory of Weak-Light Nonlinear Photonics, Ministry of Education, School of Physics, Nankai University, Tianjin 300071, China. *E-mail: lwu@nankai.edu.cn.

[b]School of Physics and Optoelectronic Engineering, Guangdong University of Technology, Guangzhou, Guangdong 510006, China.

[c]Institute of Urban Environment, Chinese Academy of Sciences, Xiamen 361021, China. *E-mail: hwzhang@iue.ac.cn.

[d]Multi-Discipline Research Center, Institute of High Energy Physics, Chinese Academy of Sciences, Beijing 100049, China. *E-mail: zhenglr@ihep.ac.cn.

[e]Tianjin Key Laboratory of Photo-electronic Thin Film Devices and Technology, College of Electronic Information and Optical Engineering, and Renewable Energy Conversion and Storage Center, Nankai University, Tianjin 300071, China.

Material preparation and characterization

Materials and synthesis: High temperature solid state method was used to synthesize $KZn(PO_3)_3:x$Mn (x = 0–1) phosphors. Analytical purity K_2CO_3, ZnO, $NH_4H_2PO_4$, and MnO_2 were ground in a mortar, followed by sintering at 500 °C or 620 °C for 20 h in ambient atmosphere in a muffle furnace. The block samples were ground to powders after cooling to room temperature. In order to compare with the non-reductive phosphors, half of the obtained samples were sintered at 500 °C or 620 °C for 6 h in H_2 (15%)–Ar (85%) atmosphere.

Characterization: The DSC curves were recorded on a Differential Scanning Calorimetry (TGA/DSC1, Mettler Toledo, Switzerland) with the alumina crucible as the vessels. Both the heating rate and the cooling rate were 10 °C min^{-1}. The X-ray diffractometer (X'Pert Pro, PANalytical B.V., Netherlands) was used to detect the phase of the powders. The

temperature-dependent XRD data were recorded on a Bruker-D8 X-ray diffractometer (Germany). The XRD data for structural refinements were collected over a 2θ range from 10° to 120° at intervals of 0.02° with a counting time of 0.5 s per step and further analysed using a software TOPAS 5. The TEM images of the crystals were obtained on a JEM-2010 microscopy (JEOL, Japan) at 200 kV. The morphologies of powder samples were characterized by a scanning electron microscope (SEM, SU8020, HITACHI, Japan) equipped with an energy dispersive X-ray spectroscopy (EDS, EMAX, HORIBA). The particle sizes of the powder samples were analyzed on the laser particle size analyzer (Mastersizer 2000, Malvin, England). The XPS spectra were collected on a Thermo Scientific ESCALAB 250Xi (America), and all obtained spectra were calibrated to a C 1s electron peak at 284.8 eV. The EPR spectra were performed by an EPR spectrometer (EMX-6/1, BRUKER, Germany). The XAFS spectra were measured by means of the 1W1B beamline (Beijing Synchrotron Radiation Facility) using transmission mode, and the energy was adjusted *via* a Mn metal foil. The XAFS data were analyzed *via* IFEFFIT/SIXPACK.

The photoluminescence excitation, emission spectra and decay curves were carried out by means of a spectrofluorimeter (FSP920, Edinburgh Instruments, England). The powder samples were compacted and excited by a 150 W Xe lamp, and the emission light was detected by a photomultiplier (R928P). The ML spectra were monitored by a grating spectrometer (SR-500i-B1, ANDOR, England). Because of the reaction between the powder samples and the epoxy resin, the stress-ML and friction-ML spectra were obtained by compressing and scratching the bulk samples. In order to study the ML intensity and decay time under different magnitudes of force, the compacted powder tablets were put on a quartz glass plate, and a steel ball fell freely from different heights to the samples *via* a guiding circular tube. A photodiode connected to a digital storage oscilloscope (MDO3024, Tektronix, America) was placed under the glass to detect the decay curves of ML. The afterglow decay curves were monitored by a FLS980 spectrofluorimeter after irradiated at 365 nm UV light

for 20 min. The TL curves were performed on a thermoluminescent meter (FJ427A1, CNCS, China) after irradiated at 365 nm UV light for 10 min.

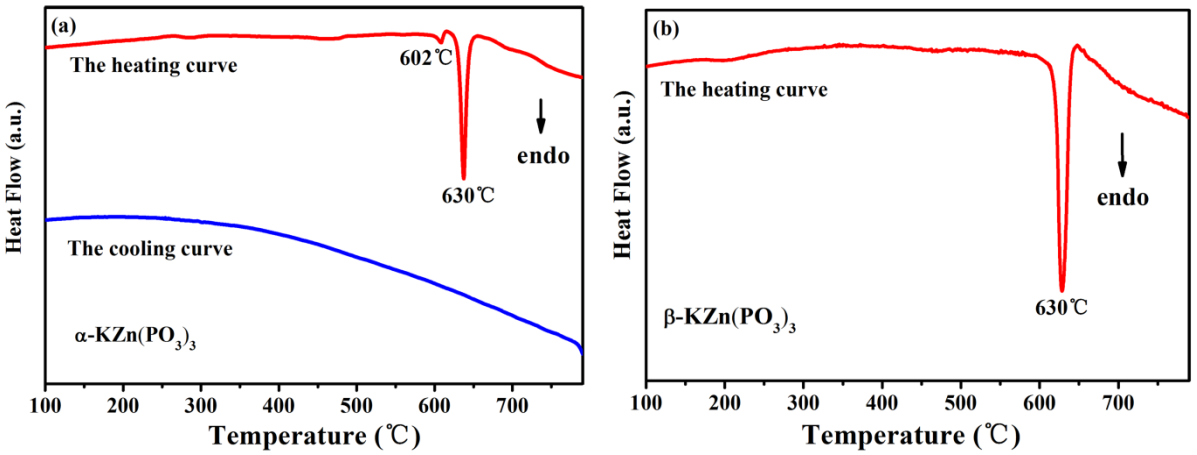

Fig. S1 The DSC curves of α-KZPO and β-KZPO, respectively.

Table S1 Lattice parameters and agreement factors for α-KZPOM$_{0.1}$ refined by Rietveld method.

Chemical formula	$K(Zn_{0.9}Mn_{0.1})(PO_3)_3$
Formula weight	340.376
Crystal system	Trigonal
Space group	*R*32
a/Å	10.1954(10)
c/Å	6.9810(3)
Cell volume/Å^3	628.43(13)
Z	3
d_c/g cm^{-3}	2.706
Diffractometer	Bruker-D8
Radiation type	Cu-Kα
Wavelength (Å)	1.5406
Profile range (°2θ)	10–120
Step size (°2θ)	0.02
No. of reflections	260 (Kα1 + Kα2)
No. of refined parameters	22
R_p (%)	5.51
R_{wp} (%)	7.44
R_{exp} (%)	5.09
χ^2	1.46

Table S2 Fractional atomic coordinates and equivalent isotropic displacement parameters (Å) for α-KZPOM$_{0.1}$ together with the occupancy.

Atom	Site	x	y	z	Occupancy
K	3b	0	0	0.5	1.0
Zn	3a	0	0	0	0.9027
Mn	3a	0	0	0	0.0973
P	9e	0.433(2)	0	0.5	1.0
O1	18f	0.1903(4)	0.1065(3)	0.1897(5)	1.0
O2	9d	0.3264(8)	0	0	1.0

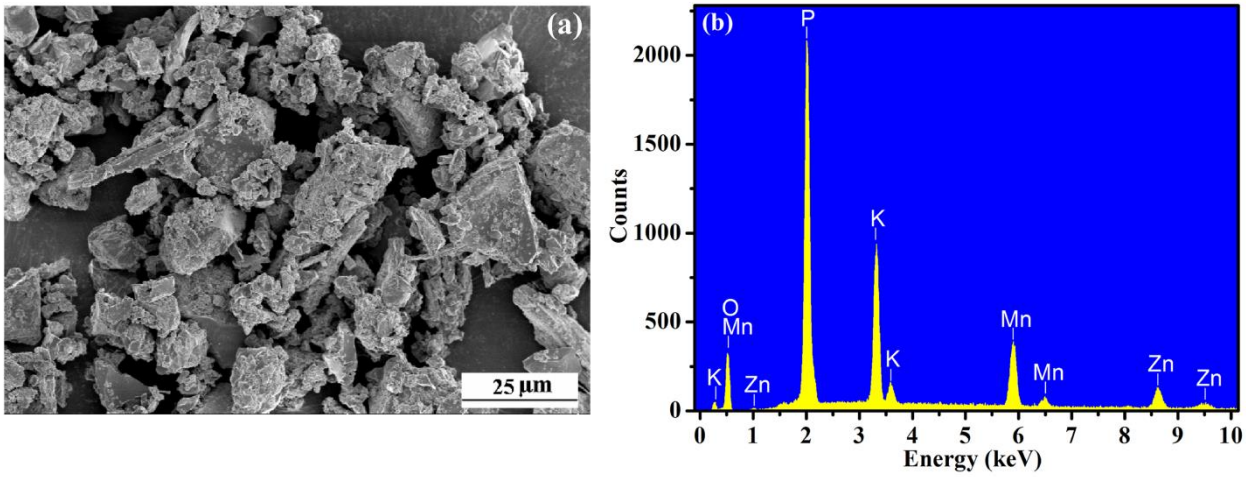

Fig. S2 (a) SEM image of α-KZPOM$_{0.3}$. (b) EDS analysis of α-KZPOM$_{0.3}$ detected in the selected square area in Fig. 3 (c).

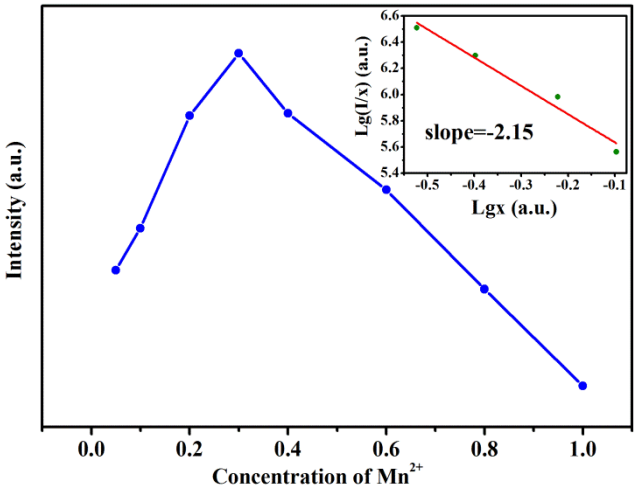

Fig. S3 The emission intensity versus Mn^{2+} concentration of α-KZPOM$_x$. The inset is the relationship between $lg(I/x)$ and $lg(x)$.

The distance between Mn^{2+} ions decreases with the increase of Mn^{2+} concentration. The critical distance (R_c) is given by the following equation[1]

$$R_c = 2\left[\frac{3V}{4\pi x_c N}\right]^{1/3} \quad (1)$$

where V is the unit cell volume, x_c refers to the critical concentration of Mn^{2+}, and N means the number of cation sites in each unit cell. For α-KZPOM$_x$, V = 621.5 Å^3, x_c = 0.3 and N = 3. The R_c value is about 10.966 Å, which is larger than 5 Å, indicating that multi-polar interaction results in the concentration quenching. Based on Dexter's theory, the interaction type is decided by the following equation [2]

$$\frac{I}{x} = \frac{K}{1+\beta(x)^{\frac{\theta}{3}}} \quad (2)$$

where the emission intensity is denoted by I, the concentration of activator ions is expressed by x, β and K are constants. θ = 6, 8, 10 refers to the dipole–dipole, dipole–quadrupole, and quadrupole–quadrupole interaction mechanism, respectively. According to the slope value of –2.15 from the inset, the obtained θ value is 6.4, which is close to 6, indicating that the concentration quenching of α-KZPOM$_x$ is caused by dipole–dipole interaction.

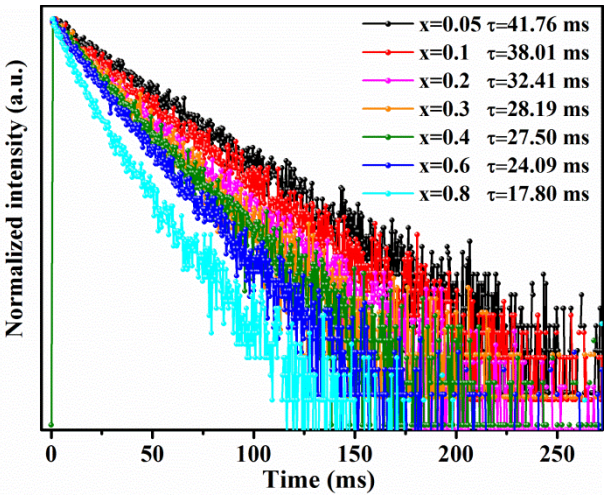

Fig. S4 The decay curves of α-KZPOM$_x$ monitored at 601nm emission wavelength.

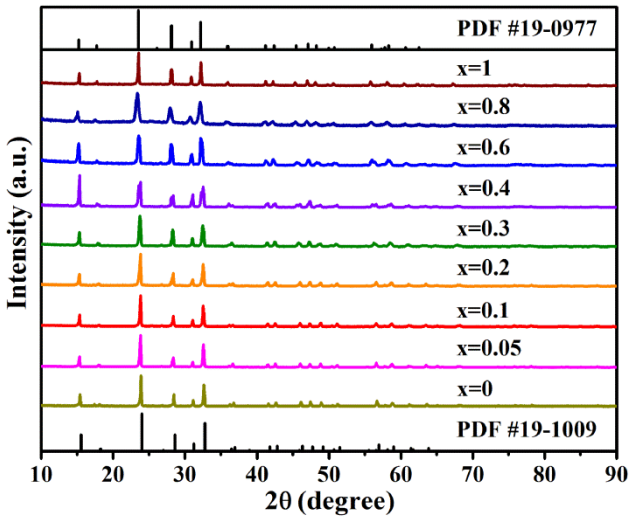

Fig. S5 The XRD patterns of β-KZPOM$_x$.

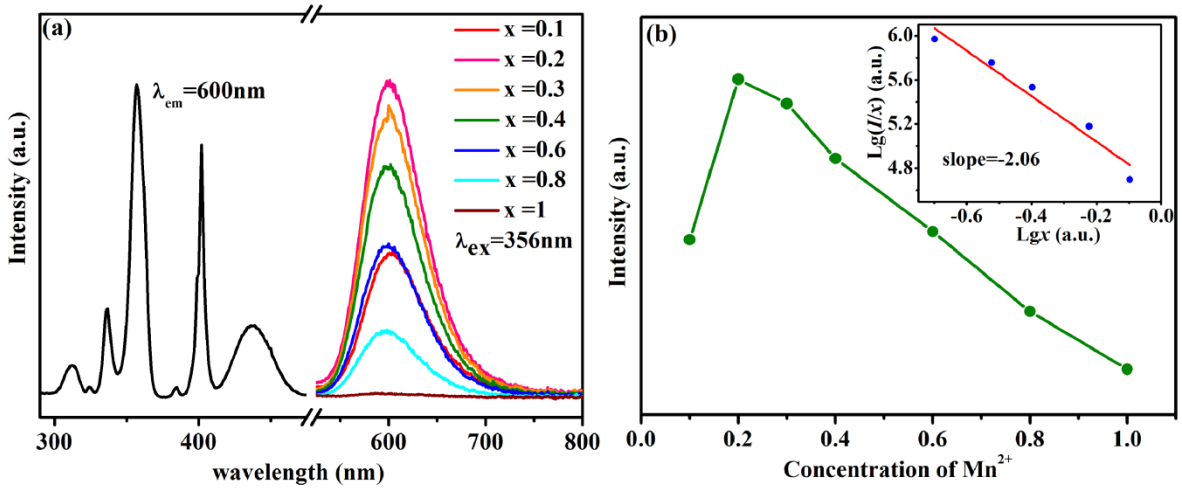

Fig. S6 (a) The PLE and PL spectra of β-KZPOM$_x$. (a) The PL intensity versus Mn^{2+} concentration of β-KZPOM$_x$.

According to the equation 2, the slope value of –2.06 from the inset, the obtained θ value is 6.18, which is close to 6, indicating that dipole–dipole interaction results in the concentration quenching of β-KZPOM$_x$.

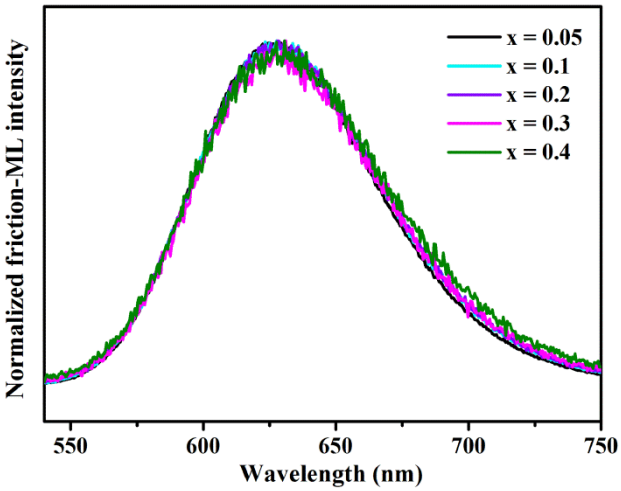

Fig. S7 The normalized friction-ML spectra of β-KZPOM$_x$.

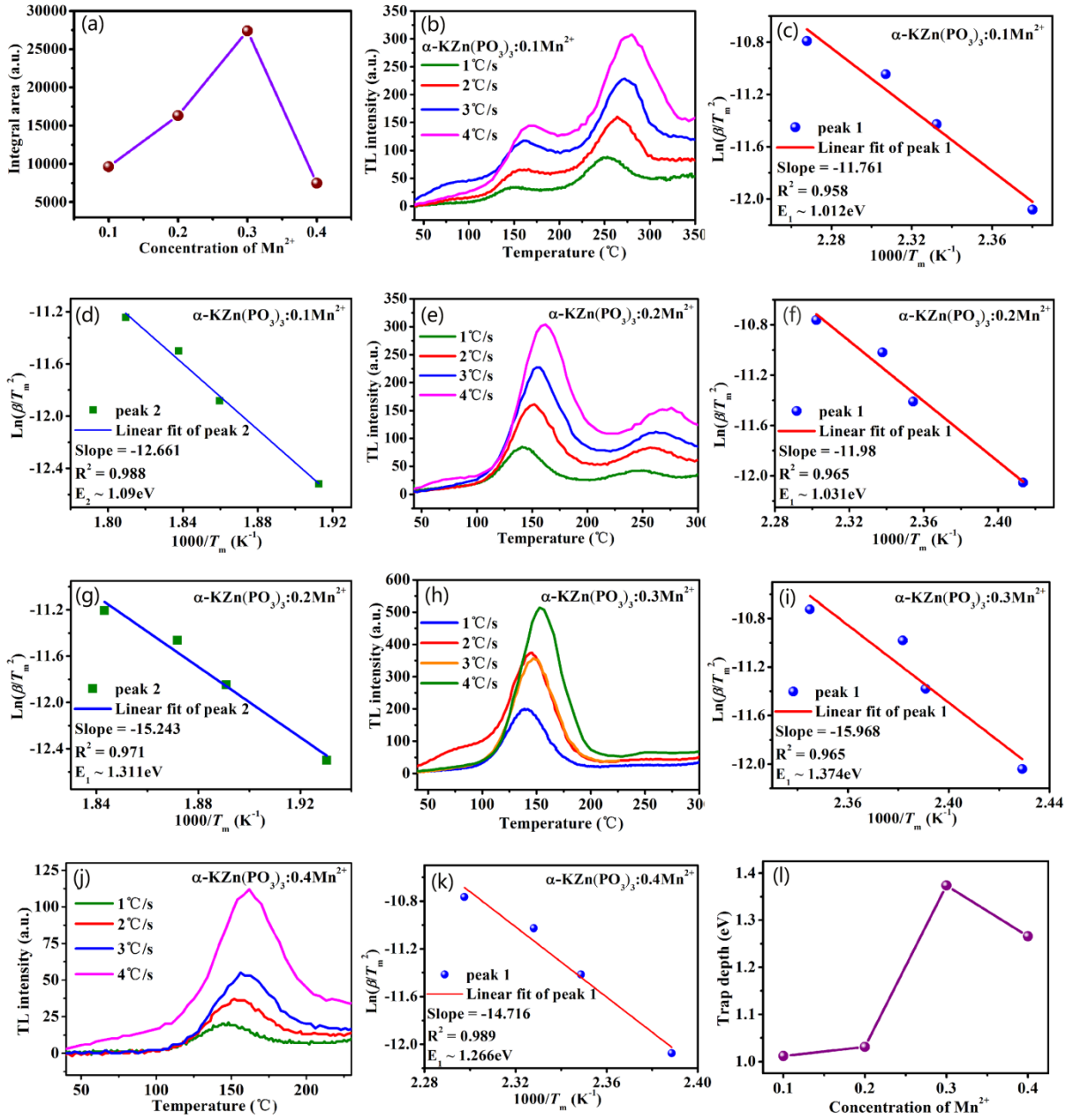

Fig. S8. (a) The integral area of Gaussian peak1. (b–k) TL curves of α-KZPOM$_x$ at different heating rate and the Hoogenstraaten plots. (l) The trap depths of E_1 versus Mn^{2+} concentration.

Supplementary Movie S1. Intense stress-ML from α-KZPOM$_{0.1}$.

References

1 G. Blasse, *Phys. Lett. A*, 1968, **28**, 444–445.

2 D. L. Dexter and J. H. Schulman, *J. Chem. Phys.*, 1954, **22**, 1063–1070.